Proc. of the Conference "Applications of Physics in Mechanical and Material Engineering" (APMME 2020)

Studies of the Magnetization Reversal Processes in Nd–Fe–B Type Magnets

I. Wnuk[a,*], A. Przybył[a] and M. Kaźmierczak[b,c]

[a] *Department of Physics, Faculty of Production Engineering and Materials Technology, Częstochowa University of Technology, al. Armii Krajowej 19, 42-200 Częstochowa, Poland*
[b] *Complex of Schools in Słupia, Primary School, Słupia 281, 28-350 Słupia Jędrzejowska, Poland*
[c] *Complex of Schools in Goleniowy, T. Kościuszki 20, 42-445 Szczekociny, Poland*

Doi: 10.12693/APhysPolA.138.166 *e-mail: wnukiza@gmail.com

In the present work the analysis of the magnetization reversal processes based on the measurements of recoil curves were studied. Two series of specimens of Nd–Fe–B-type alloy were investigated: (i) melt-spun ribbons and (ii) mechanically alloyed magnets. It was shown that in both cases annealing of the samples causes change of the magnetic properties. This is an effect of the evolution of the microstructure and phase constitution driven by the annealing. Based on the recoil curves measurements the M_{rev} (M_{irr}) curves were constructed. Furthermore, the minor hysteresis loops allowed to determine the dependences of coercivity on the maximum external magnetic field. These two approaches allowed concluding about the magnetization reversal processes.

topics: magnetic properties, nanocrystalline structure, magnetic hysteresis loop, magnetization reversal process

1. Introduction

Magnetization reversal processes are complex and some differences are visible in theoretical description of mechanisms of coercivity. The coercivity of permanent magnet is function of its internal magnetic properties and is strongly dependent on its microstructure. An occurrence of coercivity is related to magnetic anisotropy (shape and crystalline) [1]. Magnetization reversal processes are observed as nucleation or pinning. The main criterion of selection of magnetic materials is their coercivity ${}_JH_c$, remanence J_r and maximum density of magnetic energy $(BH)_{\max}$ [2]. The values of these parameters depend on chemical composition and production technique [2]. Mentioned parameters were achieved for the $Nd_2Fe_{14}B$ alloy, while its Curie temperature is relatively low (T_{C} = 585 K). One of the most goal, in the investigation of this alloy, is shift of its Curie point toward higher temperatures. A partial substitution of Fe by Nb causes an increase of the T_{C} and a field of magnetic anisotropy of prepared alloy, while results in a decrease of saturation magnetization [3–6]. The aim of the present work was to study of magnetic properties and magnetization reversal processes in the $(Nd_{10}Fe_{67}B_{23})_{95}Nb_5$ alloy.

2. Material and experimental methods

Nanocrystalline ribbons of the investigated $(Nd_{10}Fe_{67}B_{23})_{95}Nb_5$ alloy were prepared by melt-spinning method with different values of linear speed of copper wheel (5, 10, 15, and 35 m/s) under low pressure of Ar atmosphere. Then samples were sealed-off in quartz tubes under low pressure of Ar gas and annealed in wide temperature range (923–1063 K) for 5 min. An increase of linear speed of copper wheel induced a decrease of thickness of produced ribbon, and its mean values were: d = 60, 35, 25, and 20 μm, for 5, 10, 15, and 35 m/s, respectively.

3. Results and discussion

An analysis of the XRD patterns, collected for produced ribbons, revealed a coexistence of the hard magnetic $Nd_2Fe_{14}B$, paramagnetic $Nd_{1+\varepsilon}Fe_4B_4$, soft magnetic α-Fe (only for sample annealed at 1063 K) and metastable $Nd_2Fe_{23}B_3$ phases. Sample in the as-cast state was built mainly by amorphous phase ($\approx$ 85 wt%), while the rest was hard magnetic $Nd_2Fe_{14}B$ ($\approx$ 4 wt%) and paramagnetic $Nd_{1+\varepsilon}Fe_4B_4$ (11 wt%). After annealing, the content of each phase was changed and equaled $\approx$ 30 wt% for the hard magnetic $Nd_2Fe_{14}B$ and 42 wt% for paramagnetic $Nd_{1+\varepsilon}Fe_4B_4$ phase [7]. Magnetic hysteresis loops were collected for samples with thickness: 20, 25, 35, and 60 μm, using vibrating sample magnetometer working in magnetic field 2 T at room temperature. Amorphous structure of the as-cast samples was confirmed by magnetic measurements, due to the fact that hysteresis loops were typical as for soft magnetic material (${}_JH_c$ = 10 kA/m). Magnetic hysteresis loops for the $(Nd_{10}Fe_{67}B_{23})_{95}Nb_5$ alloy ribbon in the as-cast state were depicted in Fig. 1.

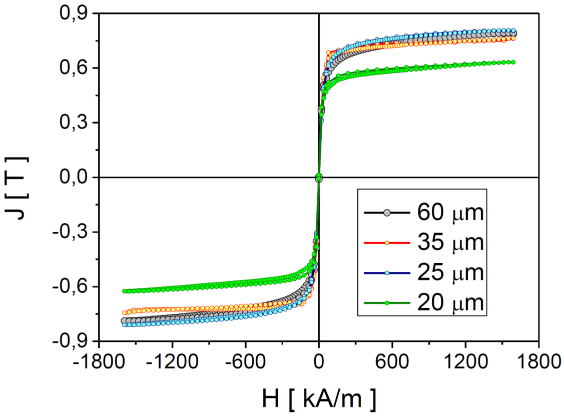

Fig. 1. Magnetic hysteresis loops for the $(Nd_{10}Fe_{67}B_{23})_{95}Nb_5$ alloy ribbons in the as-cast state prepared with different speeds of copper wheel.

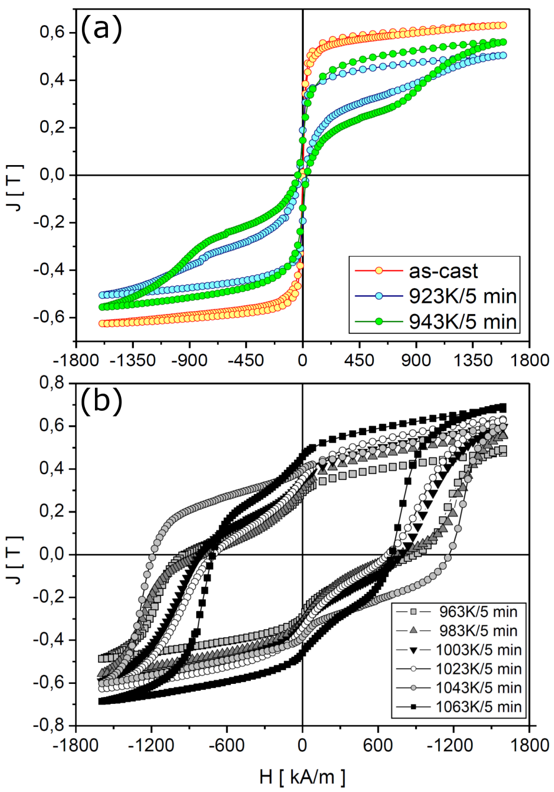

Fig. 2. Magnetic hysteresis loops for the $(Nd_{10}Fe_{67}B_{23})_{95}Nb_5$ alloy ribbon in the as-cast state and after annealing at 923 K and 943 K (a) and annealed at higher temperatures (b).

Figure 2 shows the hysteresis loops of the $(Nd_{10}Fe_{67}B_{23})_{95}Nb_5$ alloy ribbon in the as-cast state and after annealing. The ribbon in the as-cast state is soft magnetic and the shape of its hysteresis loop is typical as for amorphous materials. The annealing of sample at 923 and 943 K induces changes in the shape of hysteresis loop. Hysteresis loops have shape as wasp-waisted loop [8], which shows that ferromagnetic phases have small content

TABLE I

Magnetic parameter of prepared $(Nd_{10}Fe_{67}B_{23})_{95}Nb_5$ alloy ribbon for annealing temperatures from 963 K to 1063 K with step 20 K for 5 min

Annealing temperature [K]	J_r [T]	$_JH_c$ [kA/m]	$(BH)_{\max}$ [kJ/m^3]
963	0.288	911	10.60
983	0.35	804	15.50
1003	0.41	775	22.00
1023	0.40	690	21.75
1043	0.46	1175	24.20
1063	0.51	710	27.50

in the phase constitution of the sample. The $J(H)$ curves were measured for annealed ribbon at temperatures 923 K and 943 K and they are typical for multiphase samples. It was confirmed by X-ray diffraction (XRD) and Mössbauer spectroscopy studies [7]. Moreover, the presence of a contraction in the vicinity of coercivity is related to higher content of soft magnetic phase (amorphous matrix and metastable phase $Nd_2Fe_{23}B_3$) than hard magnetic ($Nd_2Fe_{14}B$) phase [14, 15]. In Fig. 2b, the hysteresis loops measured for sample annealed at 963 K and 1063 K were shown. While annealing temperature increased, the broadening of hysteresis loop was clearly visible and rises. It was result of an increase of content of hard magnetic phase. These samples are also multiphase, which is visible on demagnetization curves and XRD investigation [7]. Basis magnetic properties delivered by hysteresis loops were collected in Table I.

Maximum coercivity $_JH_c = (1175 \pm 12)$ kA/m was revealed for sample annealed at 1043 K, maximum density of magnetic energy $(BH)_{\max} = (27.5 \pm 2)$ kJ/m^3 and maximum saturation magnetization $J_r = (0.51 \pm 0.01)$ T were observed for sample annealed at 1063 K. Figure 3 shows magnetization virgin curves for the as-cast and annealed (at selected temperatures) $(Nd_{10}Fe_{67}B_{23})_{95}Nb_5$ alloy ribbons. The measurements were carried out for thermally demagnetized samples. Magnetization virgin curves collected for as-cast ribbons are characterized as for amorphous material.

The same shape of magnetization virgin curve was observed for sample annealed at 923 K. It corresponds well with measurements of magnetic hysteresis loops. For relatively low values of magnetic field, the sharp increase of polarization magnetization was detected. Short-time (5 min) annealing at temperatures higher than 943 K caused noticeable changes in shape of magnetization virgin curves. In Fig. 3, the characteristic inflection point is observed in magnetization virgin curves, which is typical for materials with dominant pinning of domain walls as magnetization reversal process. Moreover, the shape of virgin curves is strongly related to volume content of each phases, which

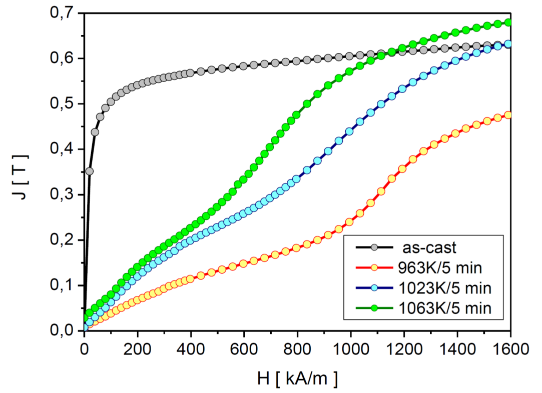

Fig. 3. Magnetization virgin curves of the $(Nd_{10}Fe_{67}B_{23})_{95}Nb_5$ alloy ribbons in the as-cast state and after annealing at selected temperatures.

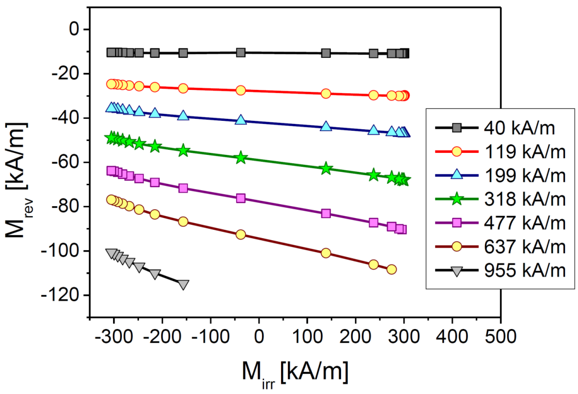

Fig. 4. The $M_{\rm rev}(M_{\rm irr})$ dependences of the $(Nd_{10}Fe_{67}B_{23})_{95}Nb_5$ alloy ribbons annealed at 983 K for 5 min.

was confirmed by XRD and Mössbauer studies [7]. In order to further analyse of magnetization reversal processes, the magnetization reversal curves were measured [9–11]. Based on these data, irreversible part of magnetization $M_{\rm irr}$ dependences of reversible part of magnetization $M_{\rm rev}$ [12] at several values of magnetic field H was constructed for sample with thickness 20 μm.

Such results, obtained for sample annealed at 983 K, were plotted in Fig. 4. Such course of the $M_{\rm rev}(M_{\rm irr})$ dependences is related to the distribution of nucleation fields H_N and pinning field H_P and degree of the overlapping of these fields [10, 13]. For nanocrystalline ribbon, the minimum of the $M_{\rm rev}(M_{\rm irr})$ curves is not observed. The course of these curves indicates that the nucleation process is started at higher values of magnetic field H, while pinning field H_P is lower than nucleation field H_N. A monotonous decrease of reversible part of magnetization $M_{\rm rev}$ with an increase of irreversible part of magnetization $M_{\rm irr}$ is observed. In order to determine magnetic interaction between grains in the $(Nd_{10}Fe_{67}B_{23})_{95}Nb_5$ alloy ribbon, $\delta M(H)$ dependences (the Henkel plot) were constructed. As was

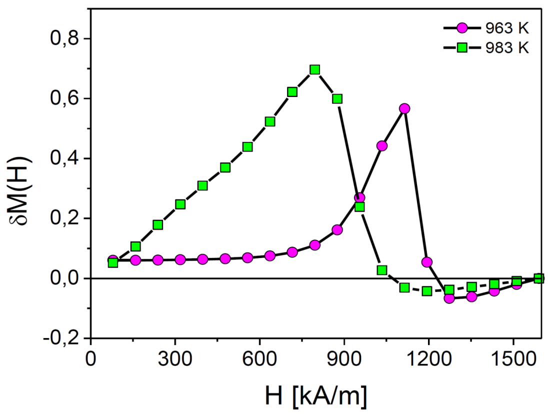

Fig. 5. The influence of annealing temperature on the shape of the $\delta M(H)$ curve of the $(Nd_{10}Fe_{67}B_{23})_{95}Nb_5$ alloy ribbon annealed at 963 K and 983 K for 5 min.

mentioned above, in studied alloy the coexistence of the following phases: $Nd_2Fe_{14}B$ and $Nd_2Fe_{23}B_3$ was confirmed and it was the reason of this analysis. Moreover, the influence of annealing temperature on the exchange interactions between soft magnetic and hard magnetic phases was investigated based on the $\delta M(H)$ dependences. The noticeable increase of characteristic maximum of the $\delta M(H)$ curve with an increase of annealing temperature was observed (Fig. 5). In the range of magnetic field 0–700 kA/m and annealing temperature 963 K, the $\delta M(H)$ is almost constant, while for annealing temperature 983 K, the sharp increase is observed. Such behavior of the δM suggests strengthening of exchange interactions between grain of each phases. Positive values of the $\delta M(H)$ are result of strong exchange interactions between $Nd_2Fe_{14}B$ and $Nd_2Fe_{23}B_3$ phases (intergrain or interlayer exchange coupling (IGEC)). Moreover, the maximum value of δM is related to energy of these interactions [11], while negative values of the δM are related to weak dipole interactions, which causes lowering of magnetization.

4. Conclusions

In the present paper the magnetic properties and magnetization reversal processes were investigated. Based on measurements of magnetic hysteresis loops, it was confirmed that samples in as cast state were soft magnetic. Heat treatment caused changes in the phase composition improved magnetic properties of prepared ribbons. The analysis of magnetic reversal processes indicated that dominant process in these materials is pinning. Moreover, the magnetization reversal processes in these alloys are strongly related to annealing temperature. Additionally, the annealing temperature had strong influence on exchange interactions between grain of phases detected in the material.

References

[1] I. Wnuk, J.J. Wysłocki, *J. Mater. Process. Technol.* **175**, 433 (2006).

[2] P. Pietrusiewicz, K. Błoch, M. Nabiałek, S. Walters, *Acta Phys. Pol. A* **127**, 397 (2015).

[3] M. Nabiałek, B. Jeż, K. Błoch, P. Pietrusiewicz, J. Gondro, *J. Magn. Magn. Mater.* **477**, 214 (2019).

[4] A Przybył, I. Wnuk, P. Gębara, J. Wysłocki, *J. Achiev. Mater. Manufact. Eng.* **49**, 210 (2011).

[5] H.R. Kirchmayr, *J. Phys. D Appl. Phys.* **29**, 2763 (1996).

[6] G. Schneider, E.Th. Henig, G. Petzow, H.H. Stadelmaier, *Zeitschr. Metallk.* **77**, 755 (1986).

[7] M. Seeger, H. Kronmüller, *Zeitschr. Metallk.* **87**, 923 (1996).

[8] I. Wnuk, A Przybył, J.J. Wysłocki, *Nukleonika* **52**, S85 (2007).

[9] I. Wnuk, M. Szwaja, *Rev. Chim.* **70**, 4450 (2019).

[10] R. O'Handley, *Modern Magnetic Materials. Principles and Applications*, Wiley, Canada 2000.

[11] D.C. Crew, L.H. Lewis, D.O. Welch, *J. Appl. Phys.* **87**, 4744 (2000).

[12] D.C. Crew, K.H. Lewis, *J. Appl. Phys.* **87**, 4783 (2000).

[13] H. Zhang, Ch. Rong, X. Du, J. Zhang, S. Zhang, B. Shen, *Appl. Phys. Lett.* **82**, 4098 (2003).

[14] D.C. Crew, P.G. McCormick, R. Street, *J. Appl. Phys.* **86**, 3278 (1999).

[15] A. Mediana-Boudri, D.R. Cornejo, O. Ayala, H.R. Bertorello, J. Matutes-Aquino, *J. Magn. Magn. Mater.* **254–255**, 219 (2003).